Study of Trajectories around a Non-Spherical Body

SILVA, A. A.[1] PRADO, A. F. B. A.[2]; WINTER, O. C.[3]
1. DSS – Space System Division
Instituto Nacional de Pesquisas Espaciais - INPE, São José dos Campos, BRAZIL.
2. DMC – Space Mechanics and Control Division
Instituto Nacional de Pesquisas Espaciais - INPE, São José dos Campos, BRAZIL.
3. DMA-FEG-UNESP – Mathematics Department – Guaratinguetá, BRAZIL.
aurea.silva@dss.inpe.br, prado@dem.inpe.br, ocwinter@feg.unesp.br
http://www.inpe.br; http://www.feg.unesp.br/

Abstract: In the present work we show the expressions of the gravitational potential of homogeneous bodies with non-spherical three-dimensional shapes in order to study the trajectories around these bodies. The potentials of prolate and oblate ellipsoids with different values of semi-major axis are presented. Their results are validated with a test using a spherical body in order to guarantee the approximation of any body as a polyhedral model. With these expressions we study trajectories of a point of mass around the three-dimensional bodies and the results indicated that the polyhedral form of the object does work very well. As a final test, we show an orbital maneuver around those bodies, using the polyhedral model for the dynamics. The results show that the best transfer was similar to the Hohmann transfer.

Keywords: Gravitational potential, non-spherical bodies, polyhedral model, tetrahedra, prolate ellipsoid, oblate ellipsoid.

1. Introduction

The purpose of the present work is to determine an analytical form to represent the potential around an irregular shaped body and to obtain a description of the possible orbital evolutions of a particle that travels around a body with those characteristics.

Conventional spherical harmonic representations of the gravitational potential of such bodies require expansions of high degree and order, which are difficult to obtain. The polyhedral method is well suited to evaluate the gravitational field of an irregularly shaped body such as asteroids, comet nucleus, and small planetary satellites. If complete coverage of the surface can be obtained, a polyhedral model of the body can be constructed. Expressions in closed forms are developed for the gravitational potential and for the acceleration due to the polyhedron with constant density. Results are developed in closed forms, instead of an infinite-series expansion, and involve only elementary functions (arc-tangent and logarithm).

The technique of the determination of the gravitational field through polyhedron is studied starting from the literature that already exist and, starting from the expressions for the polyhedron, we developed an algorithm to illustrate the equipotential surface of a non-spherical body, whose field is not known yet. The results that will be shown consist of sets of analytical equations that give the potential due to the different geometrical forms.

The polyhedral method is used to study the gravitational potential of spherical and non-spherical three-dimensional bodies (a unity radius sphere, prolate and oblate ellipsoids with different values of semi-major axis). The dynamics of the orbit of a test particle around such bodies is studied. In general, when the particle is far from the sphere, its position returns to the initial point after a Keplerian orbital period. On the other hand, when the particle gets close to its surface, the effect of its polyhedral form shows short-periodic variations in the semi major axis and eccentricity of the orbit. The results showed that the orbits close to ellipsoids become eccentric and precess due to the effects of its potential. With these results it is possible to verify that the polyhedral form of the object does work very well and this method is efficient to study trajectories. With the gravitational potential determined, an orbital evolution around the 3-D bodies can be done. The test consists on a transfer from an initial orbit to a final orbit with a minimum impulsive ΔV. More details about orbital transfers can be found in references [1] to [7]. These orbits are discretized in an ensemble of points equally spaced, generating a group of solution for the maneuver and, from this group of solutions, the best one can be found. The polyhedron expressions are an approximation to reality, since real bodies are not polyhedra and contain density irregularities, but these expressions are a good representation and can be used to study orbits around such bodies. This research generates fundamental theoretical knowledge that can be applied in irregular bodies with more complex forms, such as asteroids.

2. The Potential of the Polyhedron

The representation of the gravitational potential around a non-spherical body is made through polyhedra with constant density, involving two kinds of terms: logarithm terms due to the edges and arc tangent terms due to the faces, as discussed elsewhere [8, 9 and 10].

A polyhedron is a three-dimensional solid body whose surface consists of a number of planar faces that meet along the edges. Two faces meet at one edge and three or more faces and a like number of edges meet at each vertex [9]. The tetrahedron is the simplest polyhedron that is constructed by four triangles forming a triangular-based pyramid.

The method developed by Werner [9] begins by deriving the potential of a 3D polyhedron. It was found expressions equivalent to the potential of a 2D polygon and a 1D straight wire. Each face of the polyhedron gets its own Cartesian coordinate system with the origin in the field point.

The divergence of the vector field $\frac{1}{2}\hat{\mathbf{r}} = \mathbf{r}/2r$ with respect to the differential element's coordinates is $1/r$. This identity allow us to convert the definition of the potential U based in a volume integral to a surface integral via the Gauss Divergence Theorem, provided the density σ is constant:

$$U \equiv G\iiint_M \frac{1}{r}dm = \frac{1}{2}G\sigma\iiint_V div\,\hat{\mathbf{r}}\,dV = \frac{1}{2}G\sigma\iint_S \hat{\mathbf{n}}^T\hat{\mathbf{r}}\,dS \tag{1}$$

where $\hat{\mathbf{n}}$ is the vector normal to the surface. Initially, we separate the surface integral (Equation 1) into a sum of integrals, one per face:

$$U = \frac{1}{2}G\sigma\sum_{f\in faces}\left(\iint_S \hat{\mathbf{n}}_f^T\hat{\mathbf{r}}\,dS\right) = \frac{1}{2}G\sigma\sum_{f\in faces}\hat{\mathbf{n}}_f^T\mathbf{r}_f\iint_S\frac{1}{r}dS \tag{2}$$

The integral $\iint dS/r$ in Equation (2) express the potential of a 2D planar region *S*. Green's Theorem is used, an integral $\iint\left(z/r^3\right)dS$ appears and it is defined as ω_f. In equation (2) the potential of a 2D planar region *S* can be given by:

$$\iint_{polygon}\frac{1}{r}dS = \sum_{e\in edges}\left(\hat{\mathbf{n}}_e^f\right)^T\mathbf{r}_e^f\int_e\frac{1}{r}dS - \hat{\mathbf{n}}_f^T\mathbf{r}_f\cdot\omega_f \tag{3}$$

The potential of a planar region can be evaluated as a line integral around the boundary, where $\hat{\mathbf{n}}_f$ is the face-normal vector and $\mathbf{r}_e^f \equiv \hat{\mathbf{i}}\,x_e + \hat{\mathbf{j}}\,y_e + \hat{\mathbf{k}}\,z_e$ is a vector from the field point to some fixed point in the plane of the face.
The integral in Equation (3) is considered as the potential of a 1D straight wire. We adopt the symbol $L_e^f \equiv \int_e\frac{1}{r}ds$ for the general edge '*e*' of face '*f*'. Werner [9] shows that the definite integral can be expressed intrinsically in terms of the distances P_i and P_j of the point field and the edge length which result is:

$$\mathrm{L}_e^f \equiv \int_e\frac{1}{r}ds = ln\frac{r_i + r_j + r_{ij}}{r_i + r_j - r_{ij}}. \tag{4}$$

Using Equations (2), (3) and (4) the potential of a constant-density polyhedron is given by:

$$U = \frac{1}{2}G\sigma\sum_{e\in edges}\mathbf{r}_e^T\mathbf{E}_e\mathbf{r}_e\cdot L_e - \frac{1}{2}G\sigma\sum_{f\in faces}\mathbf{r}_f^T\mathbf{F}_f\mathbf{r}_f\cdot\omega_f \tag{5}$$

where: G is the gravitational constant; σ is the constant density; $r_{e(f)}$ is the vector from the field point to some fixed point in the edge (face); $L_e \equiv \int_e\frac{1}{r}dS$ is the vector from the field point to some fixed point in the edge (face); $F_f \equiv \hat{\mathbf{n}}_f\hat{\mathbf{n}}_f^T$ is a 3x3 matrix from each face and $E_{ij} \equiv \hat{\mathbf{n}}_A\left(\hat{\mathbf{n}}_{ij}^A\right)^T + \hat{\mathbf{n}}_B\left(\hat{\mathbf{n}}_{ji}^B\right)^T$ is a 3x3 matrix in terms of the two face-normal and edge-normal vectors.

3. Orbital Evolution around a 3-D Body

In order to test the method of polyhedron potential, one irregular body (hypothetic asteroid) is created and divided in a finite number of tetrahedron through a software called FEMAP. Each tetrahedron generates a group of 4 vertexes containing the coordinates *x*, *y*, *z* (see Fig. 1).

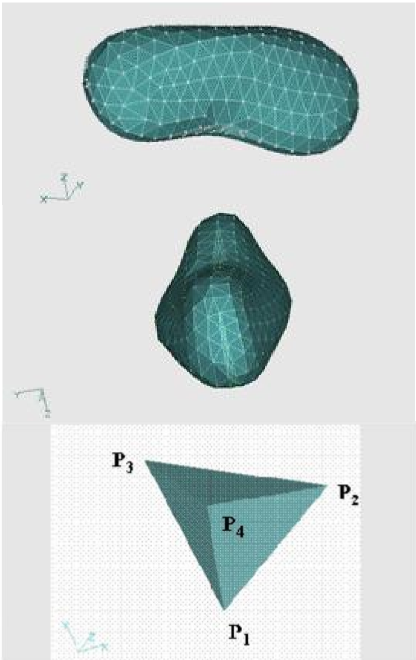

Fig. 1 – Examples of a solid divided in tetrahedra.

Equation (5) will be used to determine the potential of each tetrahedron. Then, the potentials of all tetrahedra will be added in order to have the total potential of the hypothetical asteroid or any irregular shaped body.

The first step of this study is to analyze the behavior of a particle that orbits around different solids divided into a finite number of tetrahedra. In our numerical simulation we will consider a sphere, a prolate and an oblate ellipsoid with different number of tetrahedral, as showed in Table 1.

For each solid created as a group of tetrahedra, trajectories are simulated using a Runge-Kutta numerical integrator considering different initial positions for the particle that orbits around each body. The central body is fixed considered the origin of the system. A particle with negligible mass is put in different initial positions and the integration occurs during a determined period of time, calculated by the two body problem approximation. The first case shows the orbit propagation around a unit sphere radius. After that, the central body considered was a prolate ellipsoid with the axes (1x3x1) and, finally, an oblate ellipsoid with the axes (2x1x2).

Table 1 – 3-D solid classification

Solid	Semiaxes	Number of Tetrahedra
Sphere	1	493
Prolate ellipsoid	(1 x 3 x 1)	239
Oblate ellipsoid	(2 x 1 x 2)	451

The initial conditions (position and velocity) of the particle were:

$$(X, Y, Z) = (R, 0, 0) \quad \text{and} \quad (Vx, Vy, Vz) = \left(0, 0, \sqrt{\frac{\mu}{R}}\right),$$

where μ is the product of the mass by the gravitational constant of the solid.

The numerical results consist of a group of trajectories around different solids, where the symbols in the figures are: *R* is the initial position of the particle in the *X*-axis and *T* is the number of periods given by the two-body problem.

In Figure 2 we can see that the orbit is circular and closed when the particle is distant from the body, but when it is next to the sphere ($R \leq 1.5$), the particle suffer a small perturbation by the gravitational potential due to the polyhedral shape of the body, and it causes a small change in the trajectory. It is important to note that the sphere was generated by a group of tetrahedra and it is\\does not represent the body very well, so it has some imprecision in its form that causes numerical errors that increase with the proximity of the particle from the body. However, this method is efficient to calculate the gravitational potential of irregular shaped bodies. In this particular case, the sphere was very well represented by the polyhedra. For better results it is possible to represent the body by a large number of triangular faces in its polyhedral model.

Then we simulated a group of orbits around a prolate ellipsoid with the axes (1x3x1) for different initial positions of the particle. The orbital plane considered is the *XZ* plane. The results show that the orbit is similar to the Keplerian orbit when the particle is relatively close to the body, but after an

ISBN: 978-1-61804-041-1

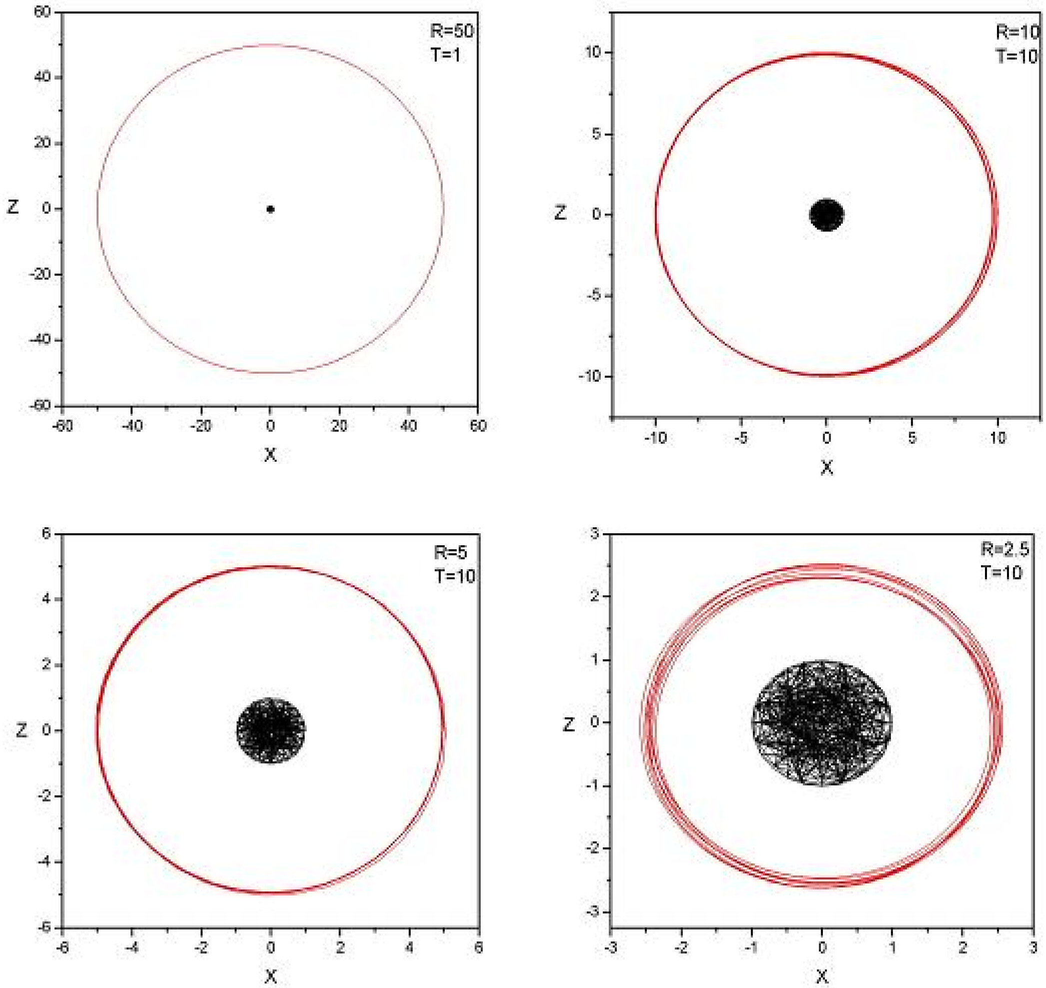
R=50
T=1
R=10
T=10
R=5
T=10
R=2.5
T=10
X
Z

4. Orbital Maneuvers

The problem of orbital maneuver consists of determining the orbital behaviour and transfer of a spatial vehicle between two given orbits. There are several factors in an orbital transference, as the control of the transference time, economy in the consumption of fuel, etc.

From the dynamic of the orbit studied, an orbital maneuver will be simulated between an internal orbit (given the initial values of position, velocity and time, respectively - R_0, V_0 and T_0) to an external orbit (given the final values of R_f, V_f and T_f) with the application of an impulse ΔV that has the smallest possible magnitude.

After each test the result will be a transfer from an initial orbit O_0 to a final orbit O_f with the minimum ΔV. The best transfer will occur from a point P_i in the internal orbit (given R_0 and V_0) to a point P_j in the external orbit (given R_f and V_f) with a minimum ΔV. The classical methods of orbital maneuvers are based in the model of impulsive propulsion. One of them is the Hohmann transfer (Prado [1]). This is a bi-impulsive solution for an optimal transfer between two circular and coplanar orbits with free time.

In this work, the method to solve this maneuver is based in the Two-Point Boundary Value Problem (TPBVP). It was chosen an initial orbit with R_0 and V_0 and a final orbit with R_f and V_f given by:

$$R_0 = \sqrt{\left(X_0^2 + Y_0^2 + Z_0^2\right)} = 5 \quad \text{and}$$

$$R_f = \sqrt{\left(X_f^2 + Y_f^2 + Z_f^2\right)} = 10.$$

The first test of an orbital maneuver considered is the one around a spherical central body. Each orbit was discretized in an ensemble of 4 points equally spaced, generating a total of 16 groups of solutions for the maneuver, in a time that varies from T_1 to T_2, where $T_1 = \frac{T_0}{4}$ (a quarter of the initial orbit) and $T_2 = T_f$, corresponding to the period of the final orbit. The group of solutions generates graphics of the velocity increment versus time ($\Delta V.vs.T$) for each group of points P_{0i} e P_{fj}. The best maneuver corresponds to the minimum point of the graphic, i.e., the minimum ΔV.

The second test considers the oblate ellipsoid as the central body. The initial and final orbits are the same ones (R_0 = 5 and R_f = 10). The minimum ΔV for this maneuver is obtained, choosing the best group of points.

Tables 2 and 3 show the ensembles of points of each discretized orbit that generated the best orbital transfer, the ΔV and the smaller time of transfer for each case.

According to the results presented in Tables 1 and 2 and Figure 6, we can verify that the best transfer for each group of points is similar to the Hohmann transfer. That analysis can be verified by calculating the values of the pericenter and apocenter of the transfer orbit (R_{per} and R_{apo}). Those values are close to the semi-major axis of the internal orbit ($R_{per} \cong 5$) and the external orbit ($R_{apo} \cong 10$). The other groups of points showed a large increment of velocity and a large time for the transfer.

For more accurate calculations we can increase the number of points in the discretization of the final and initial orbits.

Table 2 – Minimum ΔV for each group of points of the discretized orbits. The central body is represented by the Sphere.

P_{0i} / P_{fj}	ΔV	T
1 / 3	1,804	36
2 / 4	1,787	31
3 / 1	1,782	30
4 / 2	1,795	32

Table 3 – Minimum ΔV for each group of points of the discretized orbits. The central body is represented by the Oblate ellipsoid.

P_{0i} / P_{fj}	ΔV	T
1 / 3	3,481	12
2 / 4	3,583	14
3 / 1	3,369	12
4 / 2	3,305	12

Figure 3 shows the values of ΔV during a determined period of time. We can see that the point of minimum of this graphic corresponds to the minimum ΔV for a given period.

Figure 4 shows one of those orbital transfers, considering the oblate ellipsoid as the central body.

ISBN: 978-1-61804-041-1

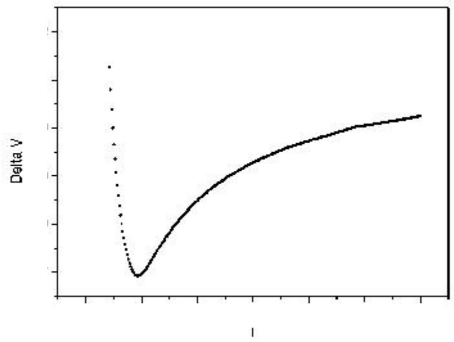

ΔV

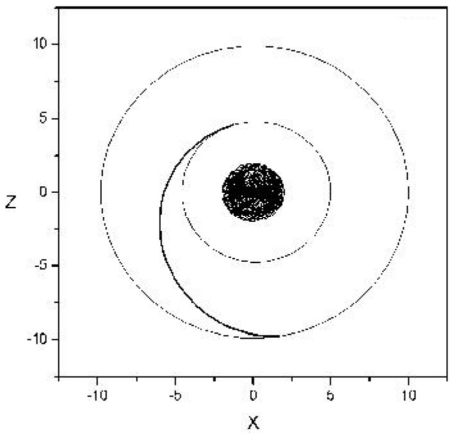

ΔV